Mass distributions in monoenergetic-neutron-induced fission of ^{238}U†

S. Nagy,* K. F. Flynn, J. E. Gindler, J. W. Meadows, and L. E. Glendenin
Argonne National Laboratory, Argonne, Illinois 60439
(Received 19 September 1977)

Fission product yields for 44 masses were determined for the fission of ^{238}U with essentially monoenergetic neutrons of 1.5, 2.0, 3.9, 5.5, 6.9, and 7.7 MeV. Fission product activities were measured by Ge(Li) γ-ray spectrometry of irradiated ^{238}U foils and by chemical separation of the fission product elements followed by β counting and/or γ-ray spectrometry. The mass-yield data for ^{238}U(n,f) show clearly the sensitive exponential increase of fission yields in the near-symmetric mass region (valley) with increasing incident neutron energy E_n (peak-to-valley ratio decreasing from ~600 to ~40) over the range E_n = 1.5 to 7.7 MeV with little change in yields in other regions of the mass distribution. The valley yields plotted semilogarithmically as a function of E_n reveal an abrupt change in slope at the onset of second-chance fission just above the neutron binding energy (at ~6 MeV) where the excitation energy is lowered by competition with neutron evaporation prior to fission. Systematics are developed to permit synthesis of the mass distribution for any neutron energy in the range of 1.5 to 18 MeV.

[NUCLEAR REACTIONS, FISSION ^{238}U(n,f) E_n =1.5, 2.0, 3.9, 5.5, 6.9, and 7.7 MeV; measured mass yields.]

I. INTRODUCTION

A survey of the literature[1] reveals a lack of data on the characteristics of fission product mass distributions for monoenergetic-neutron-induced fission (n_E,f) of ^{238}U, particularly as a function of incident neutron energy E_n. Ford and Leachman[2] determined the yields of four fission products in the near-symmetric mass region (A = 109 to 113) at seven E_n values in the range of 4.7 to 18 MeV. Borisova *et al.*[3] measured the fission yield ratios for ^{77}As, ^{111}Ag, and ^{115}Cd relative to ^{99}Mo and ^{140}Ba at nine neutron energies between 1.5 and 17.7 MeV. More complete mass-yield data were obtained for E_n = 3.0 MeV by Lyle *et al.*[4-6] (12 masses) and by Harvey *et al.*[7] (32 masses). By contrast, the mass distribution for fission of ^{238}U by 14-MeV neutrons is now well characterized by several studies reviewed in Refs. 1, 8, 9 and by more recent comprehensive work utilizing both chemical separation with β counting[10] and high-resolution γ-ray spectrometry.[8,11,12]

The present work was undertaken to explore systematically the characteristics of the mass distribution for ^{238}U(n_E,f) as a function of E_n over the range of 1.5 to 8 MeV. For this purpose reasonably complete mass distributions (44 masses) were obtained at E_n values of 1.5, 2.0, 3.9, 5.5, 6.9, and 7.7 MeV.

II. EXPERIMENTAL

A. Neutron irradiations

Targets used in the neutron irradiations were 2.54-cm diameter × 0.0127-cm thick disks of uranium metal with an average weight of 1.34 g and an isotopic composition of 99.78% ^{238}U and 0.22% ^{235}U. The attenuation of neutrons in the energy range of 1.5 to 8 MeV by a target disk was about 0.5%. Irradiations were made at the ANL Fast Neutron Generator Facility[13] in the manner described by Smith and Meadows.[14] The targets were attached to a low-mass fission chamber containing a thin, standardized deposit of ^{238}U to monitor the fission rate. This assembly was positioned about 3 cm from the neutron source. Neutrons with energies below 5 MeV were produced by the ^{7}Li(p,n)^{7}Be reaction; neutrons of higher energy were produced by the ^{2}H(d,n)^{3}He reaction.

Characteristics of the irradiations with principal neutron energies $\bar{E}_n$ of 1.5, 2.0, 3.9, 5.5, 6.9, and 7.7 MeV are presented in Table I. The spread in principal energy is caused by the thickness of the lithium or deuterium target and by the emission angle of the neutrons. The contributions to the fission rate by neutrons of other energies are also given in Table I. These neutrons arise from the ^{7}Li(p,n)^{7}Be* reaction, from deuteron stripping reactions primarily in the deuterium target cell, and from elastic and inelastic scattering by the room environment. Small corrections (1 to 7%) were made for the effects of these neutrons on the fission yields of masses that are sensitive to neutron energy (A = 109 to 129).

To optimize detection efficiency for both short- and long-lived fission products short (20 min) and longer (6–14 h) irradiations were made at each neutron energy with the exception of $\bar{E}_n$ = 6.9 MeV for which there was only a long irradiation.

TABLE I. Neutron irradiation characteristics.

Neutron source	Principal neutron energy $\bar{E}_n$ (MeV)	Energy spread (MeV)	Beam intensity (neutrons $cm^{-2} sec^{-1}$)	Fission rate in ^{238}U target ($sec^{-1} g^{-1}$) ($\times 10^4$)	Contribution to ^{238}U fission rate by neutrons of other energies E_1 [a] (%)	E_2 [b] (%)	E_3 [c] (%)
$^7Li(p,n)^7Be$	1.5	1.41–1.54	6.7×10^6	1.2	0.6		2.2
$^7Li(p,n)^7Be$	2.0	1.93–2.07	1.8×10^7	3.2	6.8		3.4
$^7Li(p,n)^7Be$	3.9	3.82–4.06	2.4×10^7	4.3	13.9		3.8
$^2H(d,n)^3He$	5.5	5.26–5.79	8.5×10^6	1.5		3.2	3.1
$^2H(d,n)^3He$	6.9	6.67–7.07	5.9×10^6	2.1		5.5	2.2
$^2H(d,n)^3He$	7.7	7.37–8.04	1.0×10^7	3.5		8.5	2.1

[a] Neutrons of approximate energy $(\bar{E}_n - 0.45)$MeV from the $^7Li(p,n)^7Be^*$ reaction.

[b] Neutrons with a broad energy spectrum averaging ~5 MeV from deuteron stripping reactions in the deuterium target cell.

[c] Neutrons with an energy spectrum from ~1 MeV to $\bar{E}_n$ arising from elastic and inelastic scattering.

B. Fission yield determinations

Fission yields were determined by high-resolution γ-ray spectrometry of an irradiated uranium target or by chemical separation of a fission product element (or group of elements) followed by γ-ray spectrometry or β counting. These three methods are designated herein as the γ, RC-γ, and RC-β methods, respectively. Yields of the rare earth and yttrium fission products were determined by both the γ and RC-γ methods. For measurement of the low activities of fission products in the near-symmetric (valley) mass region (109 to 129) and for ^{83}Br and ^{106}Ru it was necessary to employ the more sensitive RC-β method. The γ method was used for all other determinations.

For chemical separation of the fission elements, with the exception of bromine, the uranium metal targets were dissolved in a solution of concentrated hydrochloric and nitric acids containing carriers of interest. For the separation of bromine the uranium was dissolved in a solution of sodium carbonate, sodium hydroxide, hydrogen peroxide, and bromine carrier. With the exception of the group separation of the rare earths plus yttrium (RE-Y) the elements were chemically purified and samples prepared for counting according to the procedures outlined by Flynn.[15]

The RE-Y samples were separated and purified by adding cerium, barium, and bismuth carriers; precipitating and discarding barium as the sulfate and bismuth as the sulfide (for removal of radium and its descendants); precipitating cerium as the fluoride, the hydroxide, and again as the fluoride; extracting any thorium present with a 0.3 M solution of di-2-ethyl hexyl phosphoric acid in n-heptane from a 10 N nitric acid solution; and precipitating cerium as the hydroxide and finally as the oxalate. The cerium oxalate precipitate was washed with water and absolute ethanol, dried by vacuum dessication, weighed to determine the chemical yield, and counted in the γ-ray spectrometer.

Chemically purified samples of the other elements were counted in a calibrated low-background (0.5 count/min) β proportional counter.[15] The radioactive purity of each sample was verified by following its decay, generally over several half-lives. The observed β counting rate for each fission product was corrected for chemical yield, counting efficiency, decay, genetic relationships, and relative degree of saturation to give the saturation activity A_∞.

The γ-ray spectrometer system used in this work was based on an 80-cm^3 lithium-drifted germanium Ge(Li) detector with a resolution of 2.1 keV [full width at half maximum (FWHM)] for the 1.33-MeV γ ray of ^{60}Co. Pulses from the detector were amplified and fed into a 4096-channel pulse-height analyzer. The gain of the system (0.5 keV/channel) was maintained by a digital stabilizer and checked periodically with a standard source of mixed γ rays (88 to 1836 keV) of measured intensities prepared by the National Bureau of Standards (NBS). Pulses with crystal-controlled frequency were injected into the preamplifier of the Ge(Li) detector. Integration of the peak produced by the pulse generator permitted accurate determination of the live time of a counting period. Samples to be counted were mounted on flat stainless-steel plates and placed in a computer-controlled sample changer designed to ensure reproducible positioning at a distance of about 3 cm from the Ge(Li) detector. The detector was shielded from β radiation by a 0.56-cm thick beryllium absorber. The full-energy photopeak counting efficiency of the detector as a function of γ-ray energy E_γ was determined from the NBS standard source counted in the same geometry as that used for the samples.

Because of the relatively high geometric efficiency (~7%) of the counting arrangement, corrections were required for losses from the photopeak caused by γ-cascade coincidence summing in the decay of nuclides in which two or more γ-rays are emitted in coincidence. Correction factors for

TABLE II. Fission product γ decay data used in fission yield measurements.

Nuclide	Half-life	E_γ (keV)	I_γ (%)	Ref.	Nuclide	Half-life	E_γ (keV)	I_γ (%)	Ref.
$^{85}Kr^m$	4.48 h	151.2	75.5 ±0.6	17	^{133}I	20.8 h	529.9	87.3±0.2	17
^{87}Kr	76.3 min	402.6	49.5 ±1.6	17	^{134}Te	41.8 min	210.5	22.4±1.1	17
							278.0	21.8±1.1	17
^{88}Kr	2.84 h	196.3	26.0 ±1.3	17			435.1	19.0±1.3	17
^{89}Rb	15.2 min	1031.9	59±6	17			566.0	19.3±1.1	17
		1248.1	43±4	17	^{135}I	6.61 h	1038.8	7.9±0.3	17
^{91}Sr	9.6 h	653.0	12.0 [a]	18			1131.5	22.5±0.8	17
		749.8	24.0 [a]	18			1260.5	28.6±1.0	17
		1024.3	33.0 [a]	18			1457.6	8.6±0.3	17
							1678.0	9.5±0.4	17
($^{91}Y^m$) [b]	49.7 min	555.6	58.0 [a,b]	18			1791.2	7.70±0.25	17
^{92}Sr	2.71 h	1383.9	90.0 [a]	18	($^{135}Xe^m$) [b]	15.3 min	526.6	81.0±0.4	17
^{93}Y	10.2 h	267.0	6.4 [a]	18	^{138}Xe	14.2 min	258.3	31.5±1.3	17
^{94}Y	19.2 min	919.2	43	19			434.5	20.3±0.9	17
^{95}Zr	64.4 day	724.2	44.2±0.5	22	^{138}Cs	32.2 min	1435.9	76.3±1.6	17
		756.7	54.8±0.5	22	^{139}Ba	83.0 min	165.8	22.0 [a]	18
^{97}Zr	16.9 h				^{140}Ba	12.79 day	537.3	24.0 [a]	18
($^{97}Nb^m$) [b]	60 sec	743.4	98.0±0.9	17	(^{140}La) [b]	40.23 h	328.8	21.6 [a]	18
($^{97}Nb^g$) [b]	72.1 min	657.9	98.3±0.1	17			487.0	46.5 [a]	18
							815.8	24.0 [a]	18
^{99}Mo	66.0 h	140.5	5.7±0.5	17			1596.4	95.33±0.16	22
		181.1	6.52±0.19	17	^{141}Ba	18.2 min	190.3	46.0 [a]	21
		739.5	13.0±0.4	17			276.9	23.3 [a]	21
($^{99}Tc^m$) [b]	6.02 h	140.5	89.0±0.9	17			343.7	14.2 [a]	21
^{101}Tc	14.1 min	306.9	88.7 [a]	20	^{141}Ce	32.5 day	145.4	48.0±2.0	17
^{103}Ru	39.35 day	497.1	86.4±2.4	17	^{142}La	93.4 min	641.2	46.5 [a]	18
^{104}Tc	18.0 min	357.8	84.4 [a]	20	^{143}Ce	33.0 h	293.2	43.5 [a]	18
^{105}Ru	4.44 h	316.5	10.2 [a]	18	^{144}Ce	284.6 day	133.5	10.7±0.4	22
		469.4	17.5 [a]	18					
		676.3	15.0 [a]	18	^{146}Ce	14.1 min	218.3	21.0 [a]	20
		724.2	44.5 [a]	18			316.8	53.0 [a]	20
^{105}Rh	35.6 h	319.2	19.6 [a]	18	^{147}Nd	11.0 day	531.0	13.1±0.8	17
^{107}Rh	21.7 min	302.8	66.0 [a]	20	^{149}Nd	1.76 h	211.3	27.3±1.8	17
^{127}Sb	92.0 h	473.2	24.8 [a]	20	^{149}Pm	53.1 h	285.8	3.0 [a]	18
		684.9	36.8 [a]	20					
^{129}Sb	4.35 h	812.6	42.6 [a]	20	^{151}Pm	28.0 h	340.1	24.0 [a]	18
^{131}I	8.04 day	364.5	81.2±1.2	17	^{153}Sm	46.6 h	103.2	28.4 [a]	18
^{132}Te	78.2 h	228.2	88.2±0.2	17					
(^{132}I) [b]	2.30 h	522.6	16.1±0.6	17					
		630.2	13.7±0.6	17					
		667.7	98.7±0.2	17					
		772.6	76.2±1.8	17					
		954.6	18.1±0.6	17					

[a] Error of ±5% assumed.

[b] In equilibrium with the parent nuclide.

TABLE III. Fission product yields in monoenergetic-neutron-induced fission of ^{238}U. Symbols used in this table have the following meanings: γ refers to γ-ray spectrometry with a Ge(Li) detector; RC-γ refers to the same technique after chemical separation; RC-β refers to β counting after chemical separation; Y is the measured fission product yield (%) with its standard error σ. Fission yield values at each incident neutron energy opposite the mass number A are weighted averages with standard errors for the values measured by the various techniques.

		Incident neutron energy (MeV)											
Fission	Measurement	1.5		2.0		3.9		5.5		6.9		7.7	
product	technique	Y (%)	σ	Y (%)	σ	Y (%)	σ	Y (%)	σ	Y (%)	σ	Y (%)	σ
^{83}Br	RC-β	0.28	0.03	0.28	0.03			0.39	0.04				
^{85}Kr^m	γ	0.79	0.05	0.77	0.03	0.88	0.04	1.03	0.06	0.83	0.05	0.74	0.04
^{87}Kr	γ	1.60	0.10	1.57	0.07	1.78	0.08	1.90	0.11	1.47	0.11	1.82	0.09
^{88}Kr	γ	1.71	0.13	1.95	0.09	2.09	0.15	2.05	0.15	1.96	0.15	2.32	0.15
^{89}Rb	γ	2.34	0.31	2.26	0.30	2.57	0.29	2.86	0.37			2.68	0.33
^{91}Sr(Y)	γ	3.93	0.22	3.94	0.21	3.96	0.28	3.63	0.21	3.99	0.23	4.04	0.23
^{92}Sr	γ	4.18	0.24	4.10	0.23	4.24	0.25	3.96	0.25	3.68	0.23	4.23	0.27
^{93}Y	γ	4.36	0.31	4.80	0.31	4.91	0.32	4.93	0.34			5.05	0.34
	RC-γ					4.31	0.29						
A = 93						4.62	0.30						
^{94}Y	γ	4.45	0.33	4.40	0.30	5.13	0.39	5.11	0.37			4.51	0.38
^{95}Zr	γ	5.31	0.21	5.14	0.19	5.34	0.19	5.59	0.19	5.58	0.18	5.36	0.19
^{97}Zr(Nb)	γ	5.36	0.16	5.58	0.15	5.62	0.15	5.44	0.15	5.43	0.41	5.62	0.16
^{99}Mo(Tc)	γ	6.29	0.30	6.12	0.20	6.00	0.22	5.46	0.32	6.06	0.27	5.96	0.25
^{101}Tc	γ	6.41	0.56	6.45	0.49	7.08	0.51	6.53	0.55			6.79	0.46
^{103}Ru	γ	6.96	0.31	7.03	0.22	6.12	0.18	6.00	0.26	5.98	0.29	6.22	0.27
^{104}Tc	γ	5.17	0.33	4.88	0.31	4.74	0.29	4.49	0.29			4.44	0.31
^{105}Ru, Rh	γ	4.68	0.26	4.52	0.24	4.40	0.27	3.87	0.31	3.88	0.21	3.75	0.21
^{106}Ru	RC-β			2.88	0.29	2.81	0.30	3.05	0.31			3.02	0.30
^{107}Rh	γ	0.54	0.47	1.05	0.27	1.05	0.22	1.40	0.59			0.71	0.18
^{109}Pd	RC-β	0.075	0.008	0.075	0.008	0.118	0.012			0.36	0.04	0.32	0.03
^{111}Ag	RC-β			0.031	0.003	0.104	0.013	0.167	0.017	0.25	0.03	0.26	0.03
^{112}Pd	RC-β	0.028	0.006	0.026	0.003	0.057	0.017			0.20	0.04	0.20	0.04
^{113}Ag^g	RC-β	0.016	0.004	0.009	0.002	0.034	0.008	0.082	0.020				
A = 113 [a]		0.022	0.006	0.012	0.003	0.044	0.011	0.11	0.03				
^{115}Cd^g	RC-β	0.0089	0.0009	0.0105	0.0010	0.029	0.003	0.067	0.007	0.116	0.012	0.165	0.022
A = 115 [a]		0.0102	0.0014	0.0121	0.0017	0.034	0.005	0.077	0.011	0.134	0.018	0.191	0.032
^{121}Sn^g	RC-β	0.0136	0.0014	0.0139	0.0014	0.029	0.003	0.091	0.009	0.122	0.012	0.151	0.015
A = 121 [a]		0.0158	0.0022	0.0161	0.0022	0.034	0.005	0.105	0.015	0.142	0.020	0.175	0.024
^{125}Sn^g	RC-β	0.0062	0.0015	0.0082	0.0020	0.026	0.007	0.033	0.008	0.067	0.017	0.091	0.022
^{127}Sb	γ					0.19	0.02	0.40	0.04	0.45	0.03	0.53	0.06
	RC-β	0.083	0.029	0.065	0.010	0.16	0.02	0.28	0.04	0.39	0.06	0.41	0.06
A = 127						0.18	0.02	0.34	0.06	0.44	0.03	0.47	0.07
^{129}Sb	γ	0.43	0.06	0.40	0.05	0.78	0.07	1.10	0.07	0.89	0.06	1.23	0.08
	RC-β	0.28	0.04	0.38	0.05	0.61	0.09	0.74	0.11	0.92	0.14	0.92	0.14
A = 129		0.32	0.06	0.39	0.04	0.72	0.08	0.99	0.16	0.90	0.06	1.16	0.13
^{131}I	γ	3.24	0.13	3.25	0.09	3.36	0.10	3.72	0.14	3.48	0.13	3.89	0.14
^{132}Te(I)	γ	5.40	0.14	5.23	0.14	4.89	0.12	5.05	0.15	5.10	0.13	5.22	0.13
^{133}I	γ	7.15	0.22	7.12	0.21	6.95	0.25	6.77	0.20	7.10	0.19	7.04	0.20
^{134}Te	γ	8.12	0.40	7.78	0.37	7.76	0.42	7.00	0.50	7.24	0.86	7.02	0.43
^{135}I	γ	7.23	0.22	7.20	0.20	6.45	0.40	6.49	0.19	6.66	0.19	6.79	0.20
^{138}Xe, Cs	γ	5.27	0.19	5.69	0.19	5.82	0.18	5.80	0.24			5.16	0.21
^{139}Ba	γ	7.11	0.71	6.95	0.55	5.43	0.60	6.50	0.47	6.10	0.45	4.54	0.35
^{140}Ba(La)	γ	6.01	0.18	6.10	0.13	6.17	0.48	5.61	0.15	5.40	0.18	5.69	0.14
^{141}Ba, Ce	γ			5.73	0.30	5.85	0.56	5.30	0.36			5.51	0.33
^{141}Ce	RC-γ			5.55	0.36	5.64	0.32			5.07	0.36		
A = 141				5.67	0.30	5.69	0.30						
^{142}La	γ	4.69	0.29	4.66	0.29	4.85	0.28	4.58	0.28	4.37	0.23	4.35	0.26
	RC-γ									4.25	0.25		
A = 142										4.32	0.23		
^{143}Ce	γ	4.63	0.29	4.62	0.25	4.60	0.28	4.75	0.29	4.28	0.26	4.58	0.27
	RC-γ			4.71	0.29	4.74	0.29			4.17	0.25		
A = 143				4.65	0.25	4.66	0.27			4.22	0.25		
^{144}Ce	RC-γ									4.75	0.62		

TABLE III. (*Continued*)

Fission product	Measurement technique	Incident neutron energy (MeV) 1.5 Y (%)	σ	2.0 Y (%)	σ	3.9 Y (%)	σ	5.5 Y (%)	σ	6.9 Y (%)	σ	7.7 Y (%)	σ
^{146}Ce	γ	3.82	0.32	3.72	0.27	3.44	0.31	3.64	0.30			3.19	0.25
^{147}Nd	γ	2.65	0.35	2.82	0.37	2.70	0.20	2.96	0.29			2.66	0.24
	RC-γ			3.46	0.29	3.23	0.25			2.90	0.26		
$A = 147$				3.22	0.31	2.91	0.26						
^{149}Nd, Pm	γ	1.74	0.37	1.72	0.20	1.94	0.20	1.51	0.24			1.91	0.19
	RC-γ					1.95	0.24			1.75	0.27		
$A = 149$						1.94	0.20						
^{151}Pm	RC-γ			0.82	0.07	0.90	0.06			0.85	0.05		
^{153}Sm	RC-γ			0.43	0.14	0.43	0.08			0.46	0.05		

[a] Total chain yield estimated by assuming isomer ratios $(m+g)/g$ of 1.35 ± 0.14 for $^{113}Ag^{g}$ (Ref. 24), 1.16 ± 0.12 for $^{115}Cd^{g}$ (Ref. 25), and 1.16 ± 0.11 for $^{121}Sn^{g}$ (Ref. 26).

this effect were obtained from measurements of peak and total efficiencies at several γ-ray energies. For the cascading γ rays of ^{60}Co the correction was 5.5%. Cascade loss corrections for fission product γ counting data ranged from 0 to 15% and were usually less than 5%.

Correction for self-absorption of γ rays in the uranium target disk was determined by measuring the transmittance T through the disk as a function of E_γ using the NBS standard source. The self-absorption correction factor S, given by the relation

$$S = \frac{1-T}{-\ln T}, \tag{1}$$

ranged from 0.75 to 0.99 for γ rays over the E_γ range of 0.15 to 2 MeV. Estimated uncertainty (1σ) in photopeak counting efficiency for the γ ray spectrometer system over this range of E_γ varied from 5% to 2% for counting of target disks, and from 3% to 2% for counting of chemically separated samples for which no self-absorption correction was required.

To enhance statistical accuracy in the determination of the fission product γ-ray activities a large number (40–60) of γ-ray spectra were recorded over a sufficient period of time (1–2 months) to encompass the wide range of half-lives involved. These complex spectra were analyzed with the computer program GAMANAL[16] to obtain the intensities of the resolved photopeaks. The fission product γ decay data selected for use in these measurements are presented with references in Table II. The measured γ-ray activities were then sorted according to fission product and analyzed by the least-squares decay program CLSQ[23] to obtain the activities A_0 at the end of irradiation. Further corrections were made as required for cascade coincidence losses, absolute γ emission intensities I_γ (listed as photons per 100 disintegrations in Table II), genetic relationships, and degree of saturation for the irradiation to give the saturation activity A_∞.

Values of A_∞ determined by the various methods just described are related to fission yields by the expression

$$\text{fission yield} = A_\infty/\text{fission rate}. \tag{2}$$

The fission rate may be determined by counting of the ^{238}U monitor in the fission chamber or, alternatively, the fission yields may be placed on an absolute basis by normalization of the complete mass distribution to 200% total yield, the undetermined yields being interpolated or extrapolated

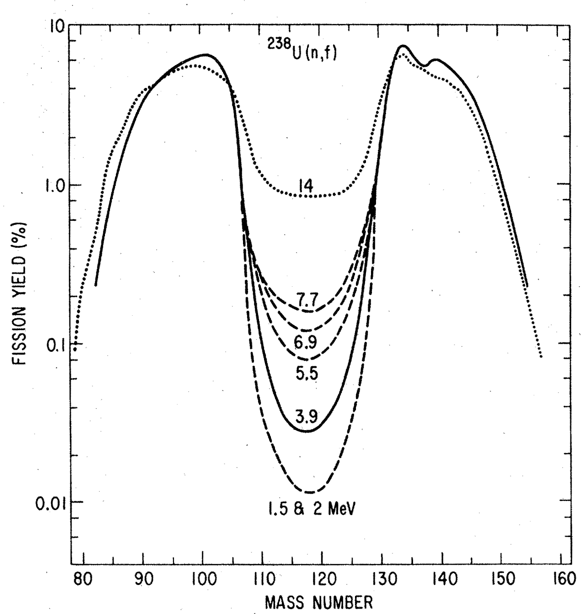

FIG. 1. Mass-yield curves for monoenergetic-neutron-induced fission of ^{238}U.

from measured yields. Since only ~30% of the total yield is undetermined, the statistical uncertainty (1σ) in the fission rate obtained by the normalization procedure is only 2% when a 20% error is assigned to all interpolated or extrapolated values. In the present work initial sets of fission yield values were obtained from the fission counting and final sets from the normalization procedure. Differences between initial and final sets of fission yields ranged from 1% to 6% for the various irradiations. The discrepancy is ascribed to small uncertainties in target position relative to the monitor caused by slight curvatures in the target disks.

III. RESULTS AND DISCUSSION

The results of the fission product yield determinations are presented in Table III and depicted graphically as mass-yield curves in Fig. 1. Uncertainties (1σ) in the fission yield values were obtained by consideration of all known sources of random error with the usual rules of error propagation. For peak fission yields (>1%) measured by the γ and RC-γ methods σ values fall typically in the range of 3 to 8%. Larger σ values ranging from 10 to 25% are associated with the valley yields measured by the RC-β method. An assessment of possible error in determination of the mass yield due to direct formation in fission (independent yield) of chain members beyond the one measured was made using the charge distribution systematics of Wolfsberg.[27] For the E_n range of 1.5 to 8 MeV calculated cumulative yields for the fission products in Table III are > 99% with the exceptions of ^{134}Te (87 to 96%) and ^{135}I (97 to 99%). The data in Table III contain no corrections for possible charge distribution effects.

As indicated by the data the peak yields for both the light and heavy mass groups are very nearly independent of E_n. The mass distribution for $E_n = 3.9$ MeV (solid curve of Fig. 1) may therefore be taken as approximately representative of the entire E_n range of 1.5 to 8 MeV for the asymmetric mass regions $A = 85$ to 106 and $A = 131$ to 153. Mass yields in the near-symmetric (valley) region ($A = 107$ to 130) for other values of E_n are shown as broken curves, with the same curve used for the similar data at $E_n = 1.5$ and 2 MeV. Also shown for comparison in Fig. 1 is the mass distribution for $E_n = 14$ MeV (dotted curve) based on the average of the fission yield data from Refs. 8, 10, 11, and 12.

The salient features apparent from the fission yield data of Table III and the mass distributions shown in Fig. 1 are (1) the strong dependence of fission yields in the valley region on E_n (increased probability of near-symmetric fission with increasing excitation energy), (2) the weak dependence of peak yields on E_n, (3) the mass shift at $E_n = 14$ MeV due to increasing neutron emission in fission with increasing excitation energy, and (4) the persistence of enhanced yield ("fine structure peak") near mass 134 at $E_n = 14$ MeV.

Yield values Y_s for the valley fission products from the present work, combined with data from the literature, are given in Table IV and plotted (semilogarithmically) as a function of E_n in Fig. 2. Also shown (at the bottom of the figure) is the cross section σ_F for neutron-induced fission of ^{238}U as a function of E_n[28] with positions indicated by arrows at approximately 6 and 14 MeV where second-chance fission (n,nf) and third-chance fission $(n,2nf)$ become energetically possible (causing steps in the σ_F curve). As evident from the plots of Y_s vs E_n the best fit to the data is obtained by separate exponential (straight line) functions for the E_n ranges associated with first-chance fission (1.5 to 6 MeV), with second-chance fission (6 to 14 MeV), and with third-chance fission (14 to 18 MeV). The data thus show clearly the effects of excitation energy on near-symmetric fission yields, i.e., an exponential increase in yield with increasing neutron energy and the abrupt breaks in slope at energies corresponding to the onset of second- and third-chance fission for which excitation energy is lowered by competition with neutron emission prior to fission. (It is of interest to note that there is essentially no change in Y_s over the E_n range of 14 to 18 MeV.) For proton-induced fission of ^{232}Th distinct dips in the Y_s curve for ^{113}Ag have been observed[29] at these points but are not seen in the present work. This may indicate that the ratio of probabilities (Γ_n/Γ_f) of neutron emission to fission for ^{238}U(n,xnf) is less than that for ^{232}Th(p,xnf).

In contrast with the energy-sensitive valley region the yields of asymmetric fission products near the peaks of the mass distribution are only slightly dependent on incident neutron energy. This is illustrated by the data for ^{99}Mo plotted at the top of Fig. 2. The fission yield is seen to decrease monotonically by only ~10% over the E_n range of 1.5 to 14 MeV, as required to compensate for the increasing yields of the valley mass region.

To obtain a more systematic and quantitative evaluation of variations in the mass distribution as a function of E_n fission yield data $Y(E_n)$ from Tables III and IV plus the averaged data for $E_n = 14$ MeV from Refs. 8, 10, 11, and 12 were fitted by the method of weighted least squares to an exponential function of the form

$$\ln Y(E_n) = \ln Y_0 + bE_n \tag{3}$$

TABLE IV. Near-symmetric fission product yields in monoenergetic-neutron-induced fission of ^{238}U.

Incident neutron energy	^{109}Pd	^{111}Ag	^{112}Pd	$^{113}Ag^{g}$	Fission product $^{115}Cd^{g}$	$^{121}Sn^{g}$	$^{125}Sn^{g}$	^{127}Sb	^{129}Sb	Ref.
1.5	0.075±0.008		0.028±0.006	0.016±0.004	0.0089±0.0009	0.0136±0.0014	0.0062±0.0015	0.083±0.029	0.32±0.06	a
1.5		0.021±0.002			0.0075±0.0008					b
2.0	0.075±0.008	0.031±0.003	0.026±0.003	0.009±0.002	0.0105±0.0010	0.0139±0.0014	0.0082±0.0020	0.065±0.010	0.39±0.04	a
2.0		0.031±0.003			0.0135±0.0014					b
3.0		0.051±0.005			0.026 ±0.003					b
3.0	0.102±0.010	0.077±0.008	0.069±0.009	0.050±0.007	0.034 ±0.006	0.051 ±0.008		0.131±0.020		c
3.9		0.089±0.009			0.047 ±0.005					b
3.9	0.118±0.012	0.104±0.013	0.057±0.017	0.034±0.008	0.029 ±0.003	0.029 ±0.003	0.026 ±0.007	0.18 ±0.02	0.72±0.08	a
4.8		0.126±0.013			0.068 ±0.007					b
5.5		0.167±0.017		0.082±0.020	0.067 ±0.007	0.091 ±0.009	0.033 ±0.008	0.34 ±0.06	0.99±0.16	a
6.9	0.36 ±0.04	0.25 ±0.03	0.20 ±0.04		0.116 ±0.012	0.122 ±0.012	0.067 ±0.017	0.44 ±0.03	0.90±0.06	a
7.7	0.32 ±0.03	0.26 ±0.03	0.20 ±0.04		0.165 ±0.022	0.151 ±0.015	0.091 ±0.022	0.47 ±0.07	1.16±0.13	a
9.1	0.55 ±0.08	0.338±0.011	0.28 ±0.03	0.187±0.005						d
13.0		0.72 ±0.08			0.57 ±0.07					e
13.4	1.14 ±0.12	1.07 ±0.11	1.09 ±0.11	0.64 ±0.07						d
14.1	1.20 ±0.06	1.08 ±0.05	1.12 ±0.05	0.66 ±0.03						d
14.8	1.25 ±0.20	0.96 ±0.12	1.00 ±0.05	1.03 ±0.08	0.95 ±0.07	0.86 ±0.14	0.96 ±0.15	1.53 ±0.15	1.65±0.13	f
14.9	1.08 ±0.03	1.07 ±0.03	1.09 ±0.04	0.666±0.018						d
15.0		0.86 ±0.10			0.78 ±0.09					e
16.4		0.95 ±0.11			0.87 ±0.10					e
17.3	1.52 ±0.12	1.12 ±0.07	0.93 ±0.04	0.73 ±0.03						d
17.7		0.80 ±0.09			0.74 ±0.09					e
18.1		1.11 ±0.05		0.86 ±0.04						d

[a] Present work.
[b] Reference 3. Ratios relative to peak yields (^{99}Mo and ^{140}Ba) normalized to peak yields from the present work.
[c] Reference 7 and personal communication.
[d] Reference 2.
[e] Reference 3. Ratios relative to peak yields normalized to the average of peak yields from Refs. 8, 10, and 12.
[f] Reference 10.

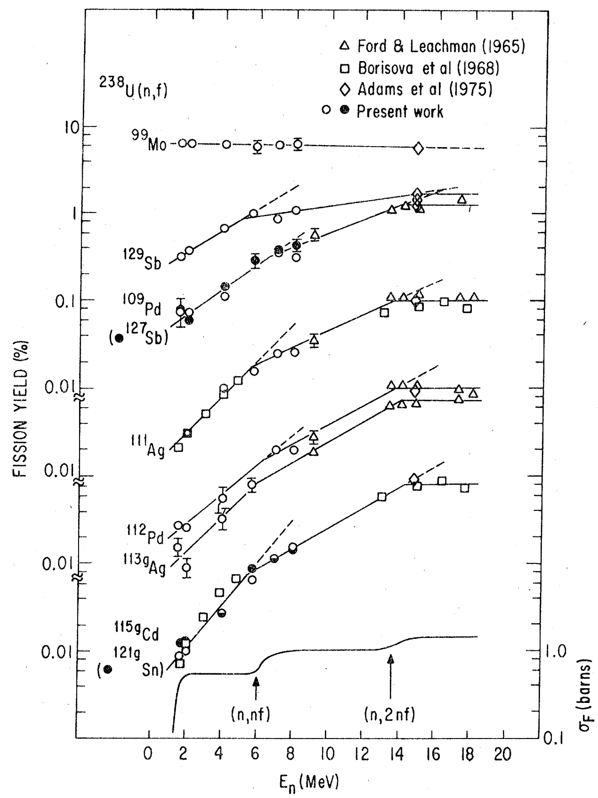

FIG. 2. Fission yields and cross section σ_F for fission of ^{238}U by monoenergetic neutrons as a function of neutron energy.

or

$$Y(E_n) = Y_0 e^{bE_n}, \tag{4}$$

where b (the slope $d\ln Y/dE_n$) is a measure of the sensitivity of fission yield to incident neutron energy. For the asymmetric mass regions ($A = 83$ to 106 and 131 to 153) the yield data for each mass were fitted to a single equation for the entire E_n range of 1.5 to 14 MeV, whereas the yield data in the valley region ($A = 109$ to 129) were divided into two ranges of E_n corresponding to first-chance fission (1.5 to 5.5 MeV) and to second-chance fission (5.5 to 14 MeV). The results are shown in Fig. 3 where b is plotted as a function of fission product mass. Data on the solid, dashed and dotted curves correspond, respectively, to the fits obtained for the three divisions of the data just described. It is seen that the asymmetric (peak) yields are only slightly sensitive to E_n, with the value of b falling in the range of ±3% per MeV for the mass range 85–106 and essentially constant at −2% per MeV for the mass range 131–153. There is a strong dependence on excitation energy for yields in the valley region, with a value for b of ~50% per MeV in the E_n range of 1.5 to 5.5 MeV for fission products near symmetry. The dependency is reduced to ~30% per MeV after the onset of second-chance fission in the E_n range of 5.5 to 14 MeV and becomes essentially zero after the onset of third-chance fission in the E_n range of 14 to 18 MeV (see Fig. 2).

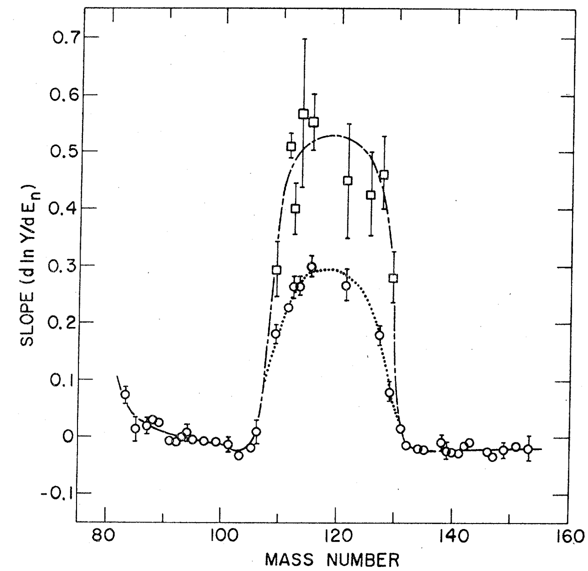

FIG. 3. The slope b in Eq. (3) as a function of fission product mass for monoenergetic-neutron-induced fission of ^{238}U.

Some mass distribution characteristics derived from the fission yield data for monoenergetic-neutron-induced fission of ^{238}U are given in Table V. The mean mass (first moment) of the light fission product group is seen to remain essentially con-

TABLE V. Mass distribution characteristics.

E_n	Peak-to-valley ratio	Mean mass (amu) Light group	Heavy group	$\bar{\nu}$ [a]	$\bar{\nu}$ [b]
1.5	600	97.5	139.0	2.5	2.60
2.0	600	97.5	139.0	2.5	2.64
3.9	200	97.4	138.9	2.7	2.94
5.5	80	97.4	138.6	3.0	3.21
6.9	50	97.5	138.4	3.1	3.41
7.7	40	97.4	138.3	3.3	3.53
14	7 [c]	98.0 [c]	136.8 [c]	4.2 [c]	4.50

[a] Calculated from conservation of mass; i.e., $\bar{\nu} = A_F - (\bar{A}_L + \bar{A}_H)$, where $\bar{\nu}$ is the average number of neutrons emitted per fission, A_F is the mass of the fissioning system (239), and $\bar{A}_L + \bar{A}_H$ is the sum of the mean masses of the light and heavy fission product groups.

[b] Experimental values based on direct measurement by fission-coincident neutron counting (Ref. 30).

[c] Based on average of fission yield data from Refs. 8, 10, 11, and 12.

stant over the E_n range of 1.5 to 7.7 MeV while the mean mass of the heavy group decreases by ~0.7 amu indicating that the increase in neutron emission per fission $\bar{\nu}$ with increasing excitation energy is primarily from the heavy fragment. Values of $\bar{\nu}$ calculated from the mean masses are in reasonable agreement with experimental values based on direct measurement by fission-coincident neutron counting[30] but are somewhat low.

From the fission yield data and systematics presented here it is now possible to synthesize with reasonable accuracy the mass distribution for monoenergetic-neutron-induced fission of ^{238}U at any value of E_n in the range of 1.5 to 18 MeV and, with the aid of the known curve[28] of σ_F vs E_n, the mass distribution for fission of ^{238}U by neutrons of any known spectrum in this energy range.

ACKNOWLEDGMENTS

The authors are indebted to A. H. Jaffey for his expert advice on error analysis. One of us (S.N.) wishes to thank the International Atomic Energy Agency for the fellowship that made possible his participation in this work and the Argonne National Laboratory for its support and hospitality.

†Work performed under the auspices of the Division of Physical Research of the U. S. Energy Research and Development Administration.

*Present address: Institute for Experimental Physics, Kossuth University, Debrecen, Hungary.

[1] J. G. Cuninghame, in *Proceedings of the Panel on Fission Product Nuclear Data* (IAEA, Vienna, 1974), Vol. 1, p. 353.

[2] G. P. Ford and R. B. Leachman, Phys. Rev. 137, 826 (1965).

[3] I. Borisova, S. M. Dubrovina, V. I. Novgorodtseva, V. A. Pchelin, V. A. Shigin, and V. M. Shubko, Yad. Fiz. 6, 454 (1967) [Sov. J. Nucl. Phys. 6, 331 (1968)].

[4] S. J. Lyle and J. Sellar, Radiochim. Acta 12, 43 (1968).

[5] S. J. Lyle and R. Wellum, Radiochim. Acta 13, 167 (1969).

[6] D. Birgul and S. J. Lyle, Radiochim. Acta 14, 103 (1970).

[7] J. T. Harvey, D. E. Adams, W. D. James, J. N. Beck, J. L. Meason, and P. K. Kuroda, J. Inorg. Nucl. Chem. 37, 2243 (1975).

[8] S. Daroczy, P. Raics, and S. Nagy, in *Proceedings of the Panel on Fission Product Nuclear Data* (see Ref. 1), Vol. 3, p. 281.

[9] M. Lammer, in *Proceedings of the Panel on Fission Product Nuclear Data* (see Ref. 1), Vol. 3, p. 245.

[10] D. E. Adams, W. D. James, J. N. Beck, and P. K. Kuroda, J. Inorg. Nucl. Chem. 37, 419 (1975).

[11] J. Blachot, L. C. Carraz, P. Cavallini, C. Chauvin, A. Ferrieu, and A. Moussa, J. Inorg. Nucl. Chem. 36, 495 (1974).

[12] M. Rajagopalan, H. S. Pruys, A. Grutter, E. A. Hermes, and H. R. von Gunten, J. Inorg. Nucl. Chem. 38, 351 (1976).

[13] S. A. Cox and P. R. Hanley, IEEE Trans. Nucl. Sci. 18, 108 (1971).

[14] D. L. Smith and J. W. Meadows, Nucl. Sci. Eng. 58, 314 (1975).

[15] K. F. Flynn, Argonne National Laboratory Report No. ANL-75-24, 1975 (unpublished).

[16] R. Gunnink and J. B. Niday, Lawrence Livermore Laboratory Report No. UCRL-51061, 1972 (unpublished).

[17] Nuclear Decay Data for Selected Radionuclides, edited by M. J. Martin, Oak Ridge National Laboratory Report No. ORNL-5114, 1976 (unpublished).

[18] R. Gunnink, J. B. Niday, R. P. Anderson, and R. A. Meyer, Lawrence Livermore Laboratory Report No. UCID-15439, 1969 (unpublished); and personal communication.

[19] C. M. Lederer, J. M. Hollander, and I. Perlman, *Table of the Isotopes* (Wiley, New York, 1967), 6th ed., p. 21.

[20] W. W. Bowman and K. W. MacMurdo, At. Data Nucl. Data Tables 13, 89 (1974).

[21] Nuclear Data Sheets 10, 151 (1973).

[22] R. G. Helmer and R. C. Greenwood, Nucl. Tech. 25, 258 (1975).

[23] J. B. Cummins, National Academy of Science-National Research Council Publication No. NAS-NS-3107, 1962 (unpublished), p. 25.

[24] K. F. Flynn, J. E. Gindler, R. K. Sjoblom, and L. E. Glendenin, Phys. Rev. C 11, 1676 (1975).

[25] M. E. Meek and B. F. Rider, Vallecitos Nuclear Center Report No. NEDO-12154-1, 1974 (unpublished).

[26] B. R. Erdal, J. C. Williams, and A. C. Wahl, J. Inorg. Nucl. Chem. 31, 2993 (1969).

[27] K. Wolfsberg, Los Alamos Scientific Laboratory Report No. LA-5553-MS, 1974 (unpublished).

[28] *Neutron Cross Sections*, compiled by J. R. Stehn, M. D. Goldberg, R. Wiener-Chasman, S. F. Mughabghab, B. A. Magurno, and V. M. May, Brookhaven National Laboratory Report No. BNL-325 (NTIS, Springfield, Va., 1965), 2nd ed., 2nd suppl., Vol. III, p. 92-238-22.

[29] B. J. Bowles, F. Brown, and J. P. Butler, Phys. Rev. 107, 751 (1957).

[30] F. Manero and V. A. Konshin, At. Energy Rev. 10, 637 (1972).